Carrier-envelope-phase insensitivity in high-order harmonic generation driven by few-cycle laser pulses

C. Hernández-García,[1,2,*] W. Holgado,[1] L. Plaja,[1] B. Alonso,[3] F. Silva,[3] M. Miranda,[3,4] H. Crespo,[3] and I. J. Sola[1]

[1]*Grupo de Investigación en Óptica Extrema, Universidad de Salamanca, E-37008, Salamanca, Spain*
[2]*JILA, University of Colorado at Boulder, Boulder, CO 80309-0440 USA*
[3]*IFIMUP-IN and Departamento de Fisica e Astronomia, Universidade do Porto, Rua do Campo Alegre 687, 4169-007 Porto, Portugal*
[4]*Department of Physics, Lund University, P.O. Box 118, SE-221 00 Lund, Sweden*
[*]*carloshergar@usal.es*

Abstract: We present evidence for self-stabilization of the relative spectral phase of high-order harmonic emission against intensity variations of the driving field. Our results demonstrate that, near the laser focus, phase matching of the harmonic field from a macroscopic target can compensate for the intensity dependence of the intrinsic phase of the harmonics emitted by a single radiator. As a consequence, we show experimentally and theoretically the insensitivity of the harmonic spectra produced at the laser focus against variations of the carrier-envelope phase (CEP) of a sub-two-cycle driving field. In addition, the associated attosecond pulse trains exhibit phase locking against CEP changes of the few-cycle driver.

OCIS codes: (190.7110) Ultrafast nonlinear optics; (190.4420) Nonlinear optics, transverse effects in; (270.6620) Strong-field processes; (320.7120) Ultrafast phenomena; (340.7480) X-rays, soft x-rays, extreme ultraviolet (EUV).

References and links

1. A. McPherson, G. Gibson, H. Jara, U. Johann, T. S. Luk, I. A. McIntyre, K. Boyer, and C. K. Rhodes, "Studies of multiphoton production of vacuum-ultraviolet radiation in the rare gases," J. Opt. Soc. Am. B **4**, 595–601 (1987).
2. M. Ferray, A. L'Huillier, X.F. Li, L.A. Lompre, G. Mainfray and C. Manus, "Multiple-harmonic conversion of 1064 nm radiation in rare gases," J. Phys. B At. Mol. Opt. Phys. **21**, L31 (1988).
3. T. Popmintchev, M. Chen, D. Popmintchev, P. Arpin, S. Brown, S. Ališauskas, G. Andriukaitis, T. Balčiunas, O. Mücke, A. Pugzlys, A. Baltuška, B. Shim, S. E. Schrauth, A. Gaeta, C. Hernández-García, L. Plaja, A. Becker, A. Jaroń-Becker, M. M. Murnane, and H. C. Kapteyn, "Bright coherent ultrahigh harmonics in the keV x-ray regime from mid-infrared femtosecond lasers," Science **336**, 1287–1291 (2012).
4. K. J. Schafer, B. Yang, L. F. DiMauro, and K. C. Kulander, "Above threshold ionization beyond the high harmonic cutoff," Phys. Rev. Lett. **70**, 1599–1602 (1993).
5. P. B. Corkum, "Plasma perspective on strong-field multiphoton ionization," Phys. Rev. Lett. **71**, 1994–1997 (1993).
6. R. López-Martens, et al., "Amplitude and phase control of attosecond light pulses," Phys. Rev. Lett. **94**, 033001 (2005).
7. P. M. Paul, E. S. Toma, P. Breger, G. Mullot, F. Augé, Ph. Balcou, H. G. Muller, and P. Agostini, "Observation of a train of attosecond pulses from high harmonic generation," Science **292**, 1689–1692 (2001).
8. C. Hernández-García, J.A. Pérez-Hernández, T. Popmintchev, M.M. Murnane, H.C. Kapteyn, A. Jaroń-Becker, A. Becker, and L. Plaja, "Zeptosecond high harmonic keV x-ray waveforms driven by midinfrared laser pulses," Phys. Rev. Lett. **111**, 033002 (2013).

#243317 Received 22 Jun 2015; revised 31 Jul 2015; accepted 2 Aug 2015; published 7 Aug 2015

9. M. B. Gaarde, J. L. Tate and K. J. Schafer, "Macroscopic aspects of attosecond pulse generation," J. Phys. B At. Mol. Opt. Phys. **41**, 132001 (2008).
10. T. Popmintchev, M.C. Chen, P. Arpin, M. M. Murnane and H. C. Kapteyn, "The attosecond nonlinear optics of bright coherent x-ray generation," Nature Photon. **4**, 822–832 (2010).
11. T. Witting, F. Frank, W. A. Okell, C. A. Arrell, J. P. Marangos, and J. W. G. Tisch, "Sub-4-fs laser pulse characterization by spatially resolved spectral shearing interferometry and attosecond streaking," J. Phys. B At. Mol. Opt. Phys. **45**, 074014 (2012).
12. E. Goulielmakis, M. Schultze, M. Hofstetter, V. S. Yakovlev, J. Gagnon, M. Uiberacker, A. L. Aquila, E. M. Gullikson, D. T. Attwood, R. Kienberger, F. Krausz, and U. Kleineberg, "Single-cycle nonlinear optics," Science **320**, 1614–1617 (2008).
13. Z. Chang, *Fundamental of Attosecond Optics* (Taylor & Francis Group, LLC, 2011).
14. G. G. Paulus, F. Grasbon, H. Walther, P. Villoresi, M. Nisoli, S. Stagira, E. Priori, and S. De Silvestri, "Absolute-phase phenomena in photoionization with few-cycle laser pulses," Nature **414**, 182–184 (2001).
15. V. Roudnev and B. D. Esry, "General theory of carrier-envelope phase effects," Phys. Rev. Lett. **99**, 220406 (2007).
16. S. Zherebtsov, F. Süßmann, C. Peltz, J. Plenge, K. J. Betsch, I. Znakovskaya, A. S. Alnaser, N. G. Johnson1,6, M. Kübel, A. Horn, V. Mondes, C. Graf, S. A. Trushin, A. Azzeer, M. J. J. Vrakking, G. G. Paulus, F. Krausz, E. Rühl, T. Fennel, and M. F. Kling, "Carrier-envelope phase-tagged imaging of the controlled electron acceleration from SiO2 nanospheres in intense few-cycle laser fields," New J. Phys. **14**, 075010 (2012).
17. D. Jones, Scott A. Diddams, Jinendra K. Ranka, Andrew Stentz, Robert S. Windeler, John L. Hall, and Steven T. Cundiff, "Carrier-envelope phase control of femtosecond mode-locked lasers and direct optical frequency synthesis," Science **288**, 635–639 (2000).
18. A. Baltuška, T. Fuji, and T. Kobayashi, "Controlling the carrier-envelope phase of ultrashort light pulses with optical parametric amplifiers," Phys. Rev. Lett. **88**, 133901 (2002).
19. F. Silva, M. Miranda, B. Alonso, J. Rauschenberger, V. Pervak, and H. Crespo, "Simultaneous compression, characterization and phase stabilization of GW-level 1.4 cycle VIS-NIR femtosecond pulses using a single dispersion-scan setup," Opt. Express **22**, 10181 (2014).
20. I. P. Christov, M. M. Murnane and H. C. Kapteyn, "High-harmonic generation of attosecond pulses in the 'single-cycle' regime," Phys. Rev. Lett. **78**, 1251–1254 (1997).
21. A. Baltuška, Th. Udem, M. Uiberacker, M. Hentschel, E. Goulielmakis, Ch. Gohle, R. Holzwarth, V. S. Yakovlev, A. Scrinzi, T. W. Hansch, and F. Krausz, "Attosecond control of electronic processes by intense light fields," Nature **421,** 611–615 (2003).
22. R. Kienberger, Goulielmakis, M. Uiberacker, A. Baltuska, V. Yakovlev, F. Bammer, A. Scrinzi, Th. Westerwalbesloh, U. Kleineberg, U. Heinzmann, M. Drescher, and F. Krausz, "Atomic transient recorder," Nature **427**, 817–821 (2004).
23. M. Nisoli, G. Sansone, S. Stagira, S. De Silvestri, C. Vozzi, M. Pascolini, L. Poletto, P. Villoresi, and G. Tondello, "Effects of carrier-envelope phase differences of few-optical-cycle light pulses in single-shot high-order-harmonic spectra," Phys. Rev. Lett. **91**, 213905 (2003).
24. A. Borot, A. Malvache, X. Chen, A. Jullien, J.-P. Geindre, P. Audebert, G. Mourou, F. Quéré and R. Lopez-Martens, "Attosecond control of collective electron motion in plasmas," Nature Phys. **8**, 416–421 (2012).
25. C. Ott, M. Schonwald, P. Raith, A. Kaldun, G. Sansone, M. Krüger, P. Hommelhoff, Y. Patil, Y. Zhang, K. Meyer, M. Laux, and T. Pfeifer, "Strong-field spectral interferometry using the carrier-envelope phase," New J. of Phys. **15**, 073031 (2013).
26. P. Rudawski, A. Harth, C. Guo, E. Lorek, M. Miranda, C. M. Heyl, E. W. Larsen, J. Ahrens, O. Prochnow, T. Binhammer, U. Morgner, J. Mauritsson, A. LHuillier, and C. L. Arnold, "Carrier-envelope phase dependent high-order harmonic generation with a high-repetition rate OPCPA-system," Eur. Phys. J. D **69**, 70 (2015).
27. G. Sansone, C. Vozzi, S. Stagira, M. Pascolini, L. Poletto, P. Villoresi, G. Tondello, S. De Silvestri, and M. Nisoli, "Observation of carrier-envelope phase phenomena in the multi-optical-cycle regime," Phys. Rev. Lett. **92**, 113904 (2004).
28. A. S. Sandhu, E. Gagnon, A. Paul, I. Thomann, A. Lytle, T. Keep, M. M. Murnane, and H. C. Kapteyn, "Generation of sub-optical-cycle, carrier-envelope-phase-insensitive, extreme-uv pulses via nonlinear stabilization in a waveguide," Phys. Rev. A **74**, 061803(R) (2006).
29. I. Thomann, A. Bahabad, X. Liu, R. Trebino, M. M. Murnane, and H. C. Kapteyn, "Characterizing isolated attosecond pulses from hollow-core waveguides using multi-cycle driving pulses," Opt. Express , **17**, 4611–4633 (2009).
30. F. Calegari, M. Lucchini, K. S. Kim, F. Ferrari, C. Vozzi, S. Stagira, G. Sansone, and M. Nisoli, "Quantum path control in harmonic generation by temporal shaping of few-optical-cycle pulses in ionizing media," Phys. Rev. A **84**, 041802 (2011).
31. V. Pervak, I. Ahmad, M. K. Trubetskov, a V Tikhonravov, and F. Krausz, "Double-angle multilayer mirrors with smooth dispersion characteristics," Opt. Express **17**, 7943–7951 (2009).
32. B. Alonso, M. Miranda, F. Silva, V. Pervak, J. Rauschenberger, J. San Román, I. J. Sola, and H. Crespo, "Characterization of sub-two-cycle pulses from a hollow-core fiber compressor in the spatiotemporal and spatiospectral

#243317 Received 22 Jun 2015; revised 31 Jul 2015; accepted 2 Aug 2015; published 7 Aug 2015

domains," Appl. Phys. B **112**, 105–114 (2013).
33. M. Miranda, C. L. Arnold, Th. Fordell, F. Silva, B. Alonso, R. Weigand, A. LHuillier, and Helder Crespo, "Characterization of broadband few-cycle laser pulses with the d-scan technique," Opt. Express **20** (17), 18732–18743, (2012).
34. C. Hernández-García, J. A. Pérez-Hernández, J. Ramos, E. Conejero Jarque, L. Roso, and L. Plaja, "High-order harmonic propagation in gases within the discrete dipole approximation," Phys. Rev. A **82**, 022432 (2010).
35. J.A. Pérez-Hernández, L. Roso, and L. Plaja, "Harmonic generation beyond the Strong-Field Approximation: the physics behind the short-wave-infrared scaling laws," Opt. Express **17**, 9891–9903 (2009).
36. C. Hernández-García, T. Popmintchev, M. M. Murnane, H. Kapteyn, L. Plaja, A. Becker and A. Jaron-Becker, "Group velocity matching in high-order harmonic generation," *submitted*.
37. C. Hernández-García, I.J. Sola, and L. Plaja, "Signature of the transversal coherence length in high-order harmonic generation," Phys. Rev. A **88**, 043848 (2013).
38. M.-C. Chen, C. Mancuso, C. Hernández-García, F. Dollar, B. Galloway, D. Popmintchev, P. C. Huang, B. Walker, L. Plaja, A. A. Jaroń-Becker, A. Becker, M. M. Murnane, H. C. Kapteyn, and T. Popmintchev, "Generation of bright isolated attosecond soft X-ray pulses driven by multicycle midinfrared lasers," Proc. Natl. Acad. Sci. USA **111**, E2361–E2367 (2014).
39. M. Nisoli, E. Priori, G. Sansone, S. Stagira, G. Cerullo, S. De Silvestri, C. Altucci, R. Bruzzese, C. de Lisio, P. Villoresi, L. Poletto, M. Pascolini, and G. Tondello "High-brightness high-order harmonic generation by truncated Bessel beams in the sub-10-fs regime," Phys. Rev. Lett. **88**, 033902 (2002).
40. Cheng Jin and C. D. Lin, "Comparison of high-order harmonic generation of Ar using truncated Bessel and Gaussian beams," Phys. Rev. A **85**, 033423 (2012).
41. B.L. Henke, E.M. Gullikson, and J.C. Davis, "X-ray interactions: photoabsorption, scattering, transmission, and reflection at E=50-30000 eV, Z=1-92," Atomic Data and Nuclear Data Tables **54** (2), 181–342 (1993).
42. M. Lewenstein, P. Salieres, and A. LHuillier, "Phase of the atomic polarization in high-order harmonic generation," Phys. Rev. A **52**, 4747–4754 (1995).
43. M. Gaarde, F. Salin, E. Constant, Ph. Balcou, K. J. Schafer, K. C. Kulander, and A. LHuillier, "Spatiotemporal separation of high harmonic radiation into two quantum path components," Phys. Rev. A **59**, 1367–1373 (1999).
44. W. Holgado, C. Hernández-García, B. Alonso, M. Miranda, F. Silva, L. Plaja, H. Crespo, and I. J. Sola, "Continuous spectra obtained from high harmonic generation driven by multicycle laser pulses," *submitted*.

1. Introduction

High-order harmonic generation (HHG) is probably the simplest technique to obtain coherent electromagnetic radiation at the extreme ultraviolet (XUV) [1, 2] or soft X-ray regimes [3]. The underlying process can be explained semiclassically by the so-called three-step model [4, 5]. In this model, in a first step, an electron is ionized from an atom by an intense laser and is subsequently accelerated in the continuum, accumulating kinetic energy from the interaction with the field. Finally, in a last step, the electron recombines with its parent ion, generating a high-energy photon. The harmonic radiation is typically emitted twice per optical cycle, forming a train of pulses of attosecond durations [6, 7], and even showing zeptosecond structures when using long wavelength (mid-infrared) drivers [8]. As a consequence, the harmonic spectrum strongly depends on the overall interference of the attosecond pulses at the detector. On the other hand, the macroscopic harmonic signal is built from the coherent addition of the radiation emitted from each elementary source in the target (typically atoms or molecules) [9, 10].

Recent developments in Ti:Sapphire (800 nm) based laser sources have enabled producing pulses as short as a few optical cycles, with durations below 5 fs (1.9 cycles) [11, 12]. In these pulses, the intensity envelope has the temporal scale of the carrier oscillations. Therefore the carrier-envelope phase (CEP), which is the offset between the envelope and the carrier waves [13], becomes relevant in the definition of the field amplitude oscillations within the pulse. There are many physical processes that depend directly on the particular shape of the electric field in the pulse [14–16], in which the control of the CEP is necessary. As a consequence, the community has made steps to achieve CEP stabilized laser systems. The standard technique consists in broadening the spectrum of the laser pulse to at least an octave and to make it interfere with its second harmonic. The interference between the two beams provides information about the CEP [17, 18]. In this work we use an alternative system, where the oc-

#243317 Received 22 Jun 2015; revised 31 Jul 2015; accepted 2 Aug 2015; published 7 Aug 2015

tave spanning pulse obtained after hollow-core fiber (HCF) post-compression directly interferes with its second harmonic [19].

HHG being a highly nonlinear process, it is very sensitive to changes in the driving field and therefore to changes in the CEP, when working with few-cycle laser pulses. For instance, CEP is especially relevant in the generation of attosecond pulses. For an adequate CEP, few-cycle laser pulses can limit the generation of harmonics to a single recollision event, and therefore to a single attosecond pulse [20]. Therefore, a well defined and stabilized CEP is experimentally required [21, 22].

In the past years, many efforts have been made to understand the microscopic (single-atom) and macroscopic responses of the harmonic radiation to CEP variations. It has been found that, in the few-cycle regime, CEP variations strongly modify the phase of the high-order harmonics, resulting in a spectral shift of the harmonic spectrum [23–26]. In addition, the HHG contribution from the so-called *long* quantum paths exhibits higher CEP-dependence than the *short* ones [27]. The role of CEP variations with macroscopic parameters such as ionization has also been studied [28–30].

In this paper we study theoretically and experimentally the dependence of HHG with the CEP of the driving field, under different macroscopic phase-matching conditions, in a gas jet target. Surprisingly, we find that the HHG spectrum becomes quite insensitive to CEP changes when the target is located near the laser focus. Firstly, we present our experimental methods and results. Secondly, we present 3D simulations of HHG of a single emitter and a macroscopic target, corroborating the experimental results and demonstrating that the CEP insensitivity arises only for the case of a macroscopic target. Then, we proceed to discuss the results, explaining the phenomenon in terms of transversal phase-matching. Finally, we present simulations showing that the phase difference between consecutive attosecond pulses becomes also insensitive to CEP variations when the gas jet is placed near the focus position.

2. Experimental results

We use a 1-kHz Ti:Sapphire CPA amplifier (Femtolasers FemtoPower Compact PRO CEP) delivering pulses with a Fourier-transform limit of 25 fs FWHM. The output pulse is post-compressed in a hollow-core fiber (HCF), with an inner diameter of 250 micrometers and 1 meter length. The HCF is filled with argon at 1 bar. By compensating the spectral phase with 10 bounces on double-angle chirped mirrors [31] (Ultrafast Innovations GmbH, nominal GDD: -40 fs^2 per bounce, minimum reflectance: 99% from 500 to 1050 nm), 4 fs pulses with an energy of 75 μJ are routinely obtained [32].

The laser pulse is then focused by a 50 cm focal length silver mirror. This mirror is placed on a translation stage, so the position of the focus can be controlled. The pulse enters the vacuum chamber through a 0.5 mm thick fused-silica window situated close to the focusing mirror to avoid any possible nonlinear effects. High-order harmonic generation is performed on an argon gas jet (5 bar of backing pressure), coming out from a nozzle of 500 μm diameter. The pressure reached inside the vacuum chamber, where the high-order harmonics are generated, is around 5×10^{-3} mbar. A 150-nm thick aluminum foil is used to filter the IR radiation and the lower harmonics. The HHG spectra are obtained with a grazing-incidence Rowland circle XUV spectrometer (Model 248/310G, McPherson Inc.), equipped with a 1-m radius and 300 grooves/mm spherical diffraction grating. A 4-mm slit is placed 2 meters far from the target.

The variation of the CEP is obtained using a home-made system, interfering the octave spanning pulse after HCF post-compression with its second harmonic [19]. The CEP is then stabilized by acting on one of the BK7 wedges inside the beam path, obtaining a RMS measured after the chirped mirrors of less than 200 mrad in 20 seconds (time taken to measure each XUV spectrum). Pulse reconstruction is performed simultaneously [19] using d-scan technique [33].

#243317 Received 22 Jun 2015; revised 31 Jul 2015; accepted 2 Aug 2015; published 7 Aug 2015

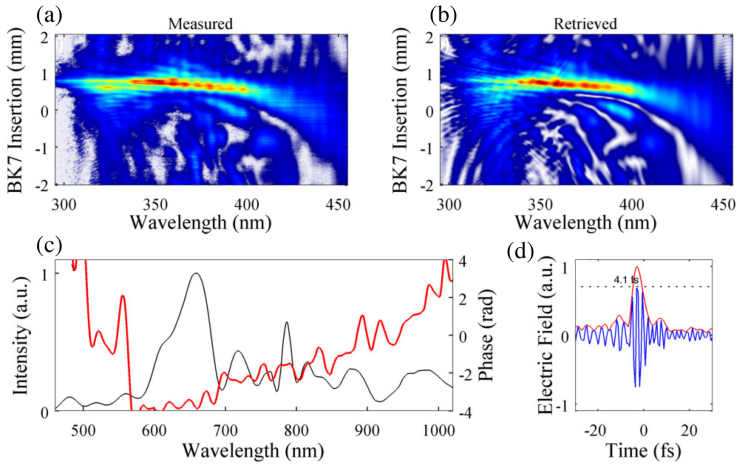

Fig. 1. D-scan traces measured (a) and retrieved (b) using d-scan technique [19]. In (c) the spectral intensity (grey) together with the spectral phase (red) is shown, while in (d) the pulse reconstructed, with a duration of 4.1 femtoseconds (fs) is presented.

Measured and retrieved d-scan traces are shown in Fig.1, as well as the spectrum and electric field of the driving pulse and its temporal duration, 4.1 fs intensity FWHM.

Figure 2 shows a systematic study of the variation of the HHG spectra with CEP, for different positions of the gas jet along the propagation direction. The experimental CEP-scans are shown in the first column of Fig. 2, where each row corresponds to the different relative positions of the gas jet respect to the focus, from (a1) z=-3 mm to (a5) z=1 mm. We observe the strongest CEP dependence of the XUV spectra in panel (a1), z=-3 mm, i.e., when the gas-jet is placed 3 millimeters before the focus position. However, when the gas-jet is placed closer to the beam focus, the dependence of the HHG spectra with CEP variations is largely reduced (see panel (a4), z=0 mm). We stress that the CEP-insensitivity is found for a CEP-locked laser system. A CEP-unlocked laser system may also show CEP-invariant harmonic spectra, coming from the average of all CEP jitter values. However, in this later case, the harmonic spectra will degenerate in a continuum structure.

3. Theoretical results

We compute high-order harmonic generation including propagation using the electromagnetic field propagator [34]. We discretize the target (gas jet) into elementary radiators, and propagate each emitted field $E_j(r,t)$ to the detector,

$$\mathbf{E}_j(\mathbf{r}_d,t) = \frac{q_j \mathbf{s}_d}{c^2|\mathbf{r}_d-\mathbf{r}_j|} \times \left[\mathbf{s}_d \times \mathbf{a}_j\left(t - \frac{|\mathbf{r}_d-\mathbf{r}_j|}{c}\right)\right] \tag{1}$$

where q_j is the charge of the electron, $\mathbf{s}_d$ is a unitary vector pointing at the detector, and $\mathbf{r}_d$ and $\mathbf{r}_j$ are the position vectors of the detector and of the elementary radiator j, respectively. The dipole acceleration $\mathbf{a}_j$ of each elementary source is computed using the SFA+ method [35], an extension of the standard Strong Field Approximation. Note that Eq. (1) assumes the harmonic radiation to propagate with the vacuum phase velocity, which is a reasonable assumption for high-order harmonics in our low-density target. The signal at the detector is computed as the coherent addition of the HHG contributions of all the elementary sources. Propagation effects of the fundamental field, including plasma and neutral dispersion as well as time-dependent

#243317 Received 22 Jun 2015; revised 31 Jul 2015; accepted 2 Aug 2015; published 7 Aug 2015

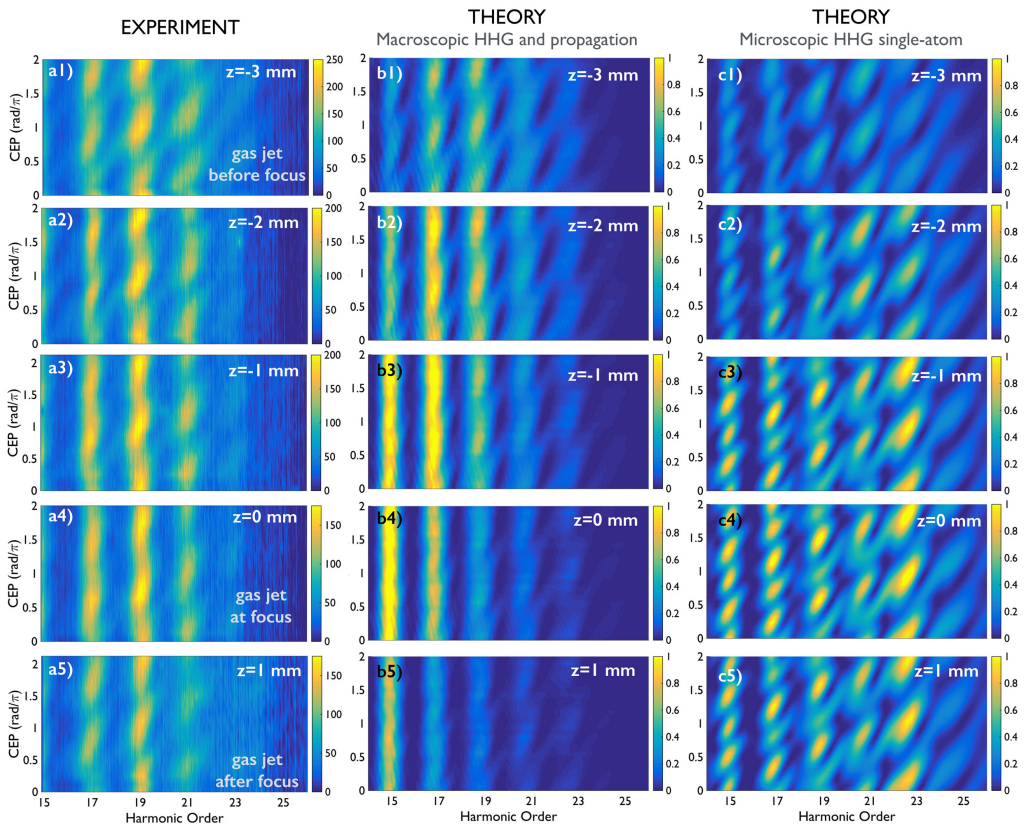

Fig. 2. CEP scans of on-axis HHG spectra for different relative positions of the gas jet and the beam focus. Each panel shows XUV spectrum intensity, versus harmonic order (x-axis) and CEP variation in π units (y-axis). The first column presents the experimental data; the second, simulations of HHG for the macroscopic target (including propagation); in the third column, results for a single-atom are presented. We show five relative positions of the gas jet and the beam focus, from z=-3 mm, where the gas jet is placed 3 mm before the focus, towards, z=1 mm, i.e., gas jet placed 1 mm after the focus position. The HHG spectra are sensitive to CEP variations when the gas jet is placed far from the focus, and becomes more insensitive near the focus.

#243317
Received 22 Jun 2015; revised 31 Jul 2015; accepted 2 Aug 2015; published 7 Aug 2015

group velocity walk-off [36] are taken into account. The absorption of the harmonics in the gas is modeled using Beer's law. The method has shown excellent agreement with experiments where phase matching is a relevant factor [3, 37, 38].

In order to reproduce the experimental conditions, we have considered a Gaussian beam propagating along the *z* direction, with a beam waist of 38 μm (Rayleigh range of 5.67 mm), focused into a transverse argon gas jet, modeled by a Gaussian density distribution along the *z* and *y* directions with 500 μm FWHM, and a constant distribution along the jet axis (*x* direction). The maximum argon density inside the gas jet is 3×10^{17} atoms/cm^3. The laser pulse envelope is modeled by a sin^2 function, with 1.8 cycles FWHM (4.5 fs), 760 nm in wavelength, and 1.7×10^{14} W/cm^2 peak intensity. The carrier is modeled as a cosine function. Note, as we will see further in the discussion, that the details of the beam profile are of secondary importance to demonstrate the CEP insensitivity. A more accurate description of the fundamental beam could be done by considering a truncated Bessel beam profile [39, 40].

In the second column of Fig. 2 we present the simulation results for the CEP-scan of on-axis high-harmonic radiation at different positions of the gas jet with respect to the laser focus: from (b1) z=-3 mm to (b5) z=1 mm. The CEP-scan is simulated by changing the delay introduced by propagating the driving laser pulse in a variable thickness of BK7 glass, mimicking the experimental procedure. The refractive index of BK7 is obtained from [41]. In the third column of Fig. 2, we present the CEP-scan of the microscopic HHG radiation generated by a single-atom placed at different positions along the laser beam propagation axis. Overall, we can observe very good agreement between experiment and the macroscopic simulations. The single-atom results, however, show a strong sensitivity to the CEP at all target positions, even at the beam focus ($z = 0$ mm). This suggests that phase-matching is behind the loss in CEP sensitivity, specially at the beam focus. Note, however, that in the single-atom results, low-order harmonics are already less sensitive to CEP variations, as it has been shown recently [26].

4. Discussion: key-role of transversal phase-matching on the observed CEP insensitivity at the focus position

According to the present understanding of HHG, high-order harmonics radiated during the recollision of the ionized electron with the parent ion form attosecond bursts of XUV radiation. The interference between these attosecond emissions conforms the HHG spectrum. Therefore, the dephasing of the subsequent attosecond bursts imprints changes in the shape of the spectrum. The intrinsic phase of a given harmonic (the phase acquired during the nonlinear HHG process) depends on the averaged intensity of the driving field over the half-cycle where the recollision takes place. CEP changes in the driving field shift the recollision times along the pulse envelope. For few-cycle pulses, the change in the intensity envelope is abrupt enough to alter noticeably the phase of the harmonic emission at the subsequent recollisions, leaving an imprint in the HHG spectrum. This explains the strong CEP sensitivity of the single-atom spectra shown in the third column of Fig. 2. The same reason holds for the results from a macroscopic target, shown in Fig. 2 for the experiment (first column) and 3D simulations (second column), as long as the target is not located near the beam focus. The surprising CEP insensitivity of the HHG spectrum at the focus, however, leads to the interesting conclusion that in the build-up of the harmonic signal in the extended target, propagation effects may compensate the phase shifts introduced by the CEP in the harmonics radiated by the single-atom source.

To gain some insight on this situation, let us compute the amplitude of the q-th order harmonic radiated during a particular electron recollision, driven by a CEP-dependent field intensity $I_0(\mathbf{r}, \phi_{CEP})$. This intensity corresponds to the square of the maximum electric field during the excursion time. In the forward direction, the far field (sum of all single-atom contributions)

#243317 Received 22 Jun 2015; revised 31 Jul 2015; accepted 2 Aug 2015; published 7 Aug 2015

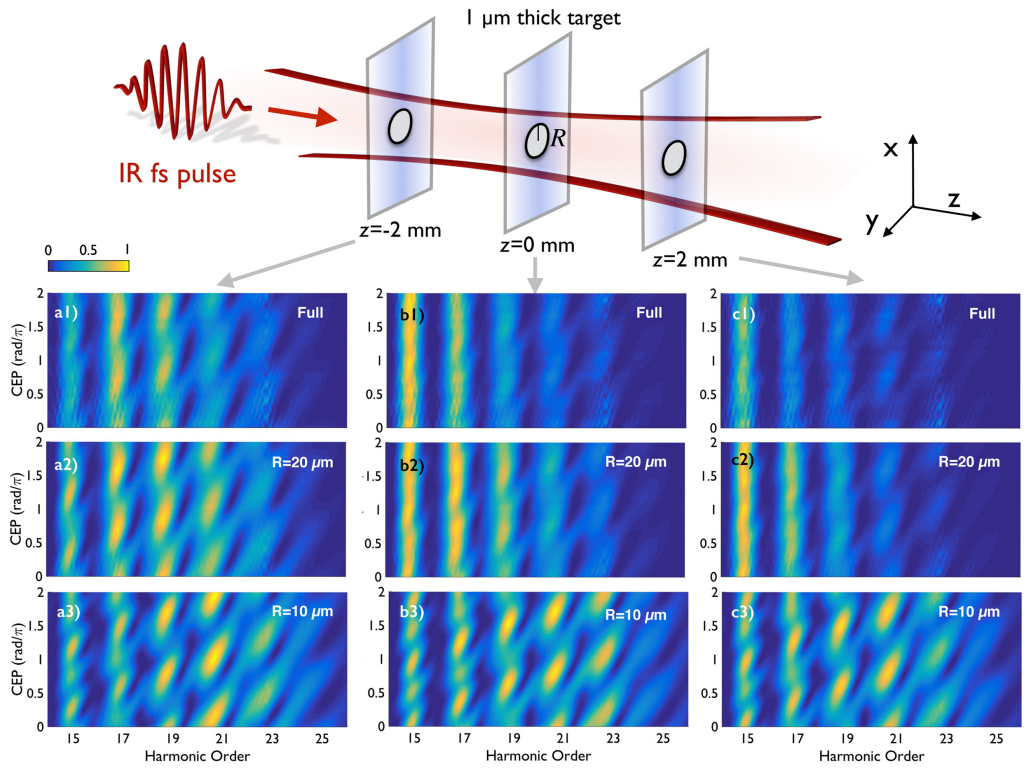

Fig. 3. Simulated CEP-scans where the longitudinal phase-matching is neglected by considering 1 μm thick targets. As depicted in the top scheme, we show different simulations where the target is clipped at different radii R. The argon gas jet is placed 2 mm before the focus position (first column) at the focus position (second column), and 2 mm after the focus position (third column). While in the first row the target is not clipped transversely, in the second and third rows it is clipped so that only radiation arising from $R < 20$ μm, and $R < 10$ μm, respectively, is considered. Note that the beam waist at focus is of 38 μm (Rayleigh range 5.67 mm). The yield is normalized in each panel.

is given by the Strong Field Approximation as

$$E_q \propto \int e^{ik(z-z_t)} n(\mathbf{r}) A_q(\mathbf{r}, \phi_{CEP}) e^{iq\phi_0(\mathbf{r},t)} e^{i\alpha I_0(\mathbf{r},\phi_{CEP})} d\mathbf{r} \tag{2}$$

where $n(\mathbf{r})$ is the target's density profile, centered at z_t. $A_q(\mathbf{r}, \phi_{CEP})$ is the amplitude modulus of the harmonic radiated at the target point $\mathbf{r}$, whose phase is given by q times the phase of the fundamental field, $\phi_0(\mathbf{r}, t)$, and the intensity-dependent intrinsic term [42, 43]. The integration over the target volume leads to constructive interference only for the emissions at the regions where the elementary radiators are coherently phase-matched. Our calculations show that the results shown in Fig. 2 are not essentially modified for targets with different lengths, as long as they are thin compared with the Rayleigh length, while the CEP insensitivity disappears if the target is clipped in the transversal direction. To support this conclusion, we represent in the first row of Fig. 3 the HHG spectra resulting from CEP-scans for a 1 μm thick target, placed (a1) 2 mm before the focus position, (b1) at the focus position and (c1) 2 mm after the focus position. Similarly as in the case with a thicker target (Fig. 2), CEP affects the HHG spectrum when the target is located out of the beam focus, while at the focus insensitivity to the CEP is

#243317 Received 22 Jun 2015; revised 31 Jul 2015; accepted 2 Aug 2015; published 7 Aug 2015

observed. The second and third rows show the same results, now clipping the target at different radii R (shown in the scheme at the top of the figure), so only the radiation of the target around the propagation axis at $R < 20$ and $R < 10$ microns, respectively, is considered. It becomes apparent how the CEP insensitivity at the focus appears for wider targets, while thinner targets show a behavior similar to the single-atom case in the third column of Fig. 2. (Note that the overall shift of the CEP-scan structure between figures 2a3 and 2c3 reflects the effect of the Gouy phase). Therefore the mechanism responsible for CEP insensitivity is mainly connected with transversal phase matching [37].

Then we may simplify Eq. (2) by considering an infinitely thin target located at the coordinate z_t.

$$E_q(z_t,\phi_{CEP}) \propto \int n(\rho,z_t)A_q(\rho,z_t,\phi_{CEP})e^{iq\phi_0(\rho,z_t,,t)}e^{i\alpha I_0(\rho,z_t,,\phi_{CEP})}\rho d\rho \tag{3}$$

The main contributions to the radial integral are those with stationary phase, given by the condition

$$\frac{\partial}{\partial\rho}\left[-qk\frac{\rho^2}{2R(z_t)}+\alpha I_0(\rho,z_t,\phi_{CEP})\right]=0 \tag{4}$$

where we have assumed a Gaussian profile for the fundamental field, with intensity $I_0(\rho,z_t,\phi_{CEP}) = I_0(z_t,\phi_{CEP})\exp\left[-2\rho^2/W^2(z_t)\right]$, and phase $\phi_0 = k\rho^2/2R(z_t)+\phi_G(z_t)$, with $W(z_t)$ the beam width, $R(z_t)$ the wavefront radius of curvature and $\phi_G(z_t)$ the Gouy phase. All radial contributions that do not fulfill Eq. (4), are not phase-matched, and therefore, will contribute weakly to the total harmonic yield. Equation (4) corresponds to the condition of optimal transverse phase matching [37] and has two solutions, the beam center $\rho^c_{st}=0$, and an annular ring given by

$$[\rho^r_{st}]^2 = -\frac{W^2(z_t)}{2}\ln\left[-\frac{q}{2\alpha I_0(z_t,\phi_{CEP})}\frac{z_t}{z_R}\right] \tag{5}$$

where z_R is the Rayleigh length, and where we have used that $W^2(z_t)/R(z_t) = \lambda z_t/\pi z_R$. Figure 4(a) shows the stationary radius as a function of the target position, for the 17th harmonic, the driving laser parameters used in Fig. 2 and the strong-field parameter, $\alpha = 1.45\times10^{-14}\,\mathrm{cm}^2/\mathrm{W}$, found from the action of the associated classical trajectories with recollision energies leading to the harmonic order considered [9]. Complex radii appear in those situations in which the stationary condition is not fulfilled. The figure demonstrates, therefore, that transversal phase matching is possible near the laser focus, and that in these cases the annular phase-matched region has a radius similar to the beam width. Substituting (5) into the Gaussian beam intensity profile $I_0(\rho,z_t,\phi_{CEP})$ above, we find that

$$\alpha I_0(\rho^r_{st},z_t,\phi_{CEP}) = -q\frac{z_t}{2z_R} \tag{6}$$

If the stationary radii are well separated, Eq. (2) can be split into two independent contributions, $E_q(z_D,t_D)\simeq E^c_q(z_D,t_D)+E^r_q(z_D,t_D)$, each one with the approximate phase evaluated at the stationary points. Therefore

$$E^c_q(z_t,\phi_{CEP}) \propto \exp\left[i\alpha I_0(0,z_t,\phi_{CEP})\right] \tag{7}$$

$$E^r_q(z_t,\phi_{CEP}) \propto \exp\left[-iqk\frac{\rho^{r2}}{2R(z_t)}-iq\frac{z_t}{2z_R}\right] \tag{8}$$

Note that, while harmonics generated at the beam center ($\rho^c_{st}=0$) are still dependent of the intensity, and therefore on CEP, the harmonics generated at the ring with radius ρ^r_{st} are independent of the intensity and, therefore, invariant under CEP variations. The reason for this can

#243317 Received 22 Jun 2015; revised 31 Jul 2015; accepted 2 Aug 2015; published 7 Aug 2015

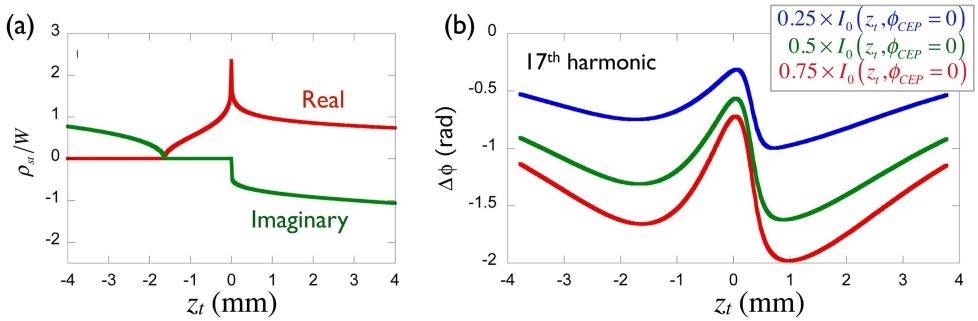

Fig. 4. (a) Real (red line) and imaginary (green line) components of the radius of the ring fulfilling the stationary phase condition, Eq. (5), for the 17th harmonic, for different positions of the target, z_t, plotted in beam width units, $W(z_t)$. (b) Phase shift of the 17th harmonic field as a function of the target location, when the driving field intensity is decreased from the maximal value $I_0(z_t,\phi_{CEP}=0)$ to $I_0(z_t,\phi_{CEP})=0.25\times I_0(z_t,\phi_{CEP}=0)$ (red line), $0.5\times I_0(z_t,\phi_{CEP}=0)$ (green line) and $0.75\times I_0(z_t,\phi_{CEP}=0)$ (blue line). The driving laser Rayleigh length is $z_R=6$ mm, intensity at the focus 1.7×10^{14} W/cm^2 and wavelength 760 nm, as in Fig. 2. The strong-field parameter $\alpha=1.45\times10^{-14}$ cm^2/W is found from the action of classical trajectories with recollision energies leading to the harmonic order considered [9].

be found in (6), which shows that the local intensity of the driving field at the ring of optimal phase matching is fixed only by the Gaussian focusing parameters. Therefore, any change of the driving field CEP forces the stationary-phase ring to accommodate to a new radius in which the local intensity remains unchanged. As a consequence, the phase-matched harmonics are always driven by the same electric field amplitude. We should stress that, in general, the two stationary points are usually not well enough separated, therefore the preceding discussion cannot be extended to a quantitative level. However, it gives enough grounds to understand the underlying mechanism for the observed CEP insensitivity.

A more accurate confirmation can be drawn from the actual numerical integration of the total field, given by Eq. (2). For simplicity we shall assume the transversal profile of the harmonic field at the target to be proportional to the profile of the fundamental beam. Also, we shall consider a flat density profile of the target. Figure 4(b) shows the phase of the 17th harmonic for different intensities and target positions z_t, using $z_R=6$ mm and intensity at the focus 1.7×10^{14}, as in Fig. 2. We shall take as reference, $\phi_{CEP}=0$, the case in which the rescattering takes place for the maximum intensity of the pulse, $I_0(z_t,\phi_{CEP}=0)=I_{max}$, therefore any change in CEP will cause a drop in the instantaneous intensity. Every colored line corresponds to the phase difference in the harmonic field found by decreasing this maximum intensity to $0.75\times I_0$, $0.5\times I_0$ and $0.25\times I_0$. The analysis clearly shows that the sensitivity of the phase of the harmonic field to variations in intensity is minimal in a rather small region around the laser focus, while being more sensitive away from this region. Our simulations point out that near the focus the harmonic emission is dominated by the annular region of the target with a stationary phase independent of the intensity, while by the beam center ($\rho_{st}^c=0$) dominates elsewhere.

As a conclusion, we have demonstrated that transversal phase-matching mitigates the HHG sensitivity to CEP variations of the few-cycle driving field under representative macroscopic conditions, and, in particular, when the target is placed at the focus position. This strongly suggests that the invariance of the HHG spectra belonging to the so-called *plateau* region in the CEP-scan is not uniquely related to the presence of long driving laser pulses.

#243317 Received 22 Jun 2015; revised 31 Jul 2015; accepted 2 Aug 2015; published 7 Aug 2015

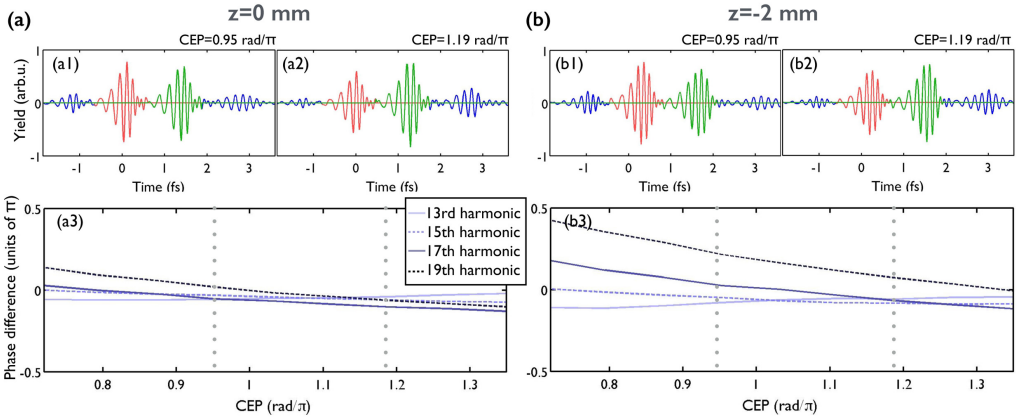

Fig. 5. Insensitivity of the attosecond pulse train phase to CEP variations of the driving field, when the gas jet is placed (a) at the focus ($z = 0$ mm) and (b) 2 mm before the focus ($z = -2$ mm). The attosecond pulse train obtained for two CEP values (0.95 and 1.19 rad/π) is presented in panels (a1)(a2) and (b1)(b2) respectively. In panels (a3) and (b3) we present the phase difference between the two main attosecond pulses (red and green lines) for different CEP variations (BK7 insertion) for the 13rd (solid light blue), 15th (dashed light blue), 17th (solid dark blue) and 19th (dashed dark blue) harmonics. When the gas jet is placed at the focus (a3) the phase difference between consecutive attosecond pulses is near zero for the different CEP, while out of focus (b3), the phase difference is larger and sensitive to CEP variations.

5. Insensitivity of the relative phase between attosecond pulses to the driving-CEP

Once we have identified the CEP insensitivity of the harmonic spectrum when the gas jet is placed at the focus position, we proceed to analyze theoretically its effect on the temporal emission. Due to the different sign of the driving electric field at each half-cycle, consecutive attosecond pulses are emitted with a global π-phase difference that results in the emission of odd-order harmonics. If the phase relation between consecutive attosecond pulses is different from π, additional spectral contributions are found [24–26], even producing a XUV continuum [44]. The results presented in Fig. 2 show that when the gas jet is placed near the focus position, the spectra is mainly composed of odd harmonics for the different values of the driving-CEP. Thus, the phase relationship between the generated attosecond pulses must be expected to be constant. On the other hand, when the gas jet is placed out of the focus, the structured CEP-scan spectra indicate that the phase relationship between consecutive attosecond pulses is strongly modified by the driving-CEP.

In Fig. 5 we present the attosecond pulse trains obtained for two CEP values (0.95 and 1.19 rad/π) when the gas jet is placed (a) at the focus ($z = 0$ mm) and (b) 2 mm before the focus ($z = -2$ mm). These temporal structures are obtained after performing the Fourier transform of the HHG spectra presented in Figs. 2(b4) and 2(b2) respectively, where an aluminum filter (150 nm in thickness) was used to filter out the low-order harmonics. In order to analyze the phase relationship between the main two attosecond pulses presented in the train (red and green lines), we extract each pulse from the train and Fourier transform them separately. The phase difference between these single-pulse spectra for different harmonic orders, from the 13th to the 19th, is plotted in Fig. 5(a3) for $z = 0$ mm and 5(b3) for $z = -2$ mm. The figure shows clearly that the spectral phase difference between two consecutive attosecond bursts remains almost constant with the harmonic order and the CEP, being nearly zero when the field is located at the

#243317 Received 22 Jun 2015; revised 31 Jul 2015; accepted 2 Aug 2015; published 7 Aug 2015

focus. However, if the gas jet is placed out of the focus, the phase difference is different from zero, and depends on the CEP of the driving field.

Therefore, attosecond pulses generated near the focus exhibit phase locking against CEP variations in the driving field. As a consequence, our results suggest that macroscopic conditions can be used to lock the relative phase between attosecond pulses in the train, without the requirement of a low-noise CEP-stabilized laser system. In Fig. 5, we observe phase-locked attosecond pulses even for a CEP jitter of 750 mrad (horizontal range of the figure), which is well above the performance of the state-of-the-art CEP stabilized laser systems employed for attoscience work (< 200 mrad).

6. Conclusions

We have analyzed the dependence of HHG with the CEP for sub-two cycle driving field aimed to a gas jet target. When the gas-jet is far from the focus, the XUV spectrum varies strongly with the CEP, while when the gas-jet is positioned near the focus position, the spectra are found to be robust against CEP variations. Theoretical analysis demonstrates that harmonics are transversally phase matched in an annular region, whose location accommodates to changes in CEP in such a way that the intrinsic phase of the harmonic field becomes insensitive to CEP variations. For the same reason, attosecond pulse trains generated near the focus exhibit phase locking against changes in CEP.

Our results show that macroscopic parameters, such as the relative position between the target and the focus, can be employed to control the CEP dependance of HHG spectra when using few-cycle pulses. This opens the possibility of minimizing the CEP dependance of the harmonics driven by few-cycle drivers, which can be useful, for example, to stabilize the generated attosecond pulse train, that can be used as a reference. Finally, these results strongly suggest that the invariance of the HHG spectra in the CEP-scan measurement is not uniquely related to the presence of long driving laser pulses.

Acknowledgments

The authors acknowledge support from MINECO (FIS2013-44174-P), from Junta de Castilla y León (Project No. SA116U13) and from Centro de Láseres Pulsados. C.H.-G. acknowledges support from the Marie Curie International Outgoing Fellowship within the EU Seventh Framework Programme for Research and Technological Development (2007-2013), under REA grant Agreement No. 328334. W.H. acknowledges ESF support through SILMI Research Networking Programme. B. A. acknowledges Fundação para a Ciência e a Tecnologia (FCT) through grant No. SFRH/BPD/88424/2012. W. H. and I. J. S. also acknowledge support from the Spanish Ministerio de Ciencia e Innovación through the Formación de Personal Investigador and Ramón y Cajal grant programs respectively. This work was partly supported by grant PTDC/FIS/122511/2010 from Fundação para a Ciência e Tecnologia, Portugal, co-funded by COMPETE and FEDER.

#243317 Received 22 Jun 2015; revised 31 Jul 2015; accepted 2 Aug 2015; published 7 Aug 2015